Hindawi Publishing Corporation
Advances in High Energy Physics
Volume 2014, Article ID 594781, 11 pages
http://dx.doi.org/10.1155/2014/594781

Research Article

Correspondence of $f(R, \nabla R)$ Modified Gravity with Scalar Field Models

Abdul Jawad[1] and Ujjal Debnath[2]

[1] *Department of Mathematics, COMSATS Institute of Information Technology, Lahore 54000, Pakistan*
[2] *Department of Mathematics, Indian Institute of Engineering Science and Technology, Shibpur, Howrah 711 103, India*

Correspondence should be addressed to Abdul Jawad; jawadab181@yahoo.com

Received 16 June 2014; Revised 11 October 2014; Accepted 11 October 2014; Published 2 November 2014

Academic Editor: Elias C. Vagenas

Copyright © 2014 A. Jawad and U. Debnath. This is an open access article distributed under the Creative Commons Attribution License, which permits unrestricted use, distribution, and reproduction in any medium, provided the original work is properly cited. The publication of this article was funded by SCOAP[3].

This paper is devoted to study the scalar field dark energy models by taking its different aspects in the framework of $f(R, \nabla R)$ gravity. We consider flat FRW universe to construct the equation of state parameter governed by $f(R, \nabla R)$ gravity. The stability of the model is discussed with the help of squared speed of sound parameter. It is found that models show quintessence behavior of the universe in stable as well as unstable modes. We also develop the correspondence of $f(R, \nabla R)$ model with some scalar field dark energy models like quintessence, tachyonic field, k-essence, dilaton, hessence, and DBI-essence. The nature of scalar fields and corresponding scalar potentials is being analyzed in $f(R, \nabla R)$ gravity graphically which show consistency with the present day observations about accelerated phenomenon.

1. Introduction

It is strongly believed that the universe is experiencing an accelerated expansion nowadays. The type Ia Supernovae [1, 2], large scale structure [3], and cosmic microwave background [4] observations have provided main evidence for this cosmic acceleration. This acceleration is caused by some unknown matter having positive energy density and negative pressure is dubbed as "dark energy" (DE). The combined analysis of cosmological observations suggests that the universe is spatially flat and consists of about 70% DE, 30% dust matter, and negligible radiations. Recent WMAP data analysis [5] also has given the confirmation of this acceleration.

The most appealing and simplest candidate for DE is the cosmological constant Λ [6–8] which has the equation of state (EoS) parameter $\omega = -1$. Over the past decade, there have been many theoretical models for mimicking DE behavior, such as Λ CDM, containing a mixture of cosmological constant Λ and cold dark matter (CDM). However, two problems arise from this scenario, namely, the "fine-tuning" and "cosmic coincidence" problems [9]. In order to solve these two problems, many dynamical DE theoretical models have been proposed [10–14].

The dynamical DE scenario is often realized by some scalar field mechanism which suggests that the energy formed with negative pressure is provided by a scalar field evolving down a proper potential. The scalar field or quintessence (a scalar field slowly evolving down its potential) [15, 16] is one of the most favored candidate of DE. Provided that the evolution of the field is slow enough, the kinetic energy density is less than the potential energy density, giving rise to the negative pressure responsible for the cosmic acceleration. A lot of scalar field DE models have been studied [17], including k-essence [10], dilaton [18], DBI-essence [19, 20], hessence [21], tachyon [11], phantom [22], ghost condensate [23, 24], and quintom [12, 25, 26]. In addition, other proposals on DE include scenarios of interacting DE models [27, 28], brane-world models [29], and Chaplygin gas models [13].

Another approach to explore the accelerated expansion of the universe is the modified theories of gravity. In this scenario, cosmic acceleration of the universe would not

arise from mysterious DE as a substance but rather from the dynamics of modified gravity. There are several models of modified gravity which include DGP brane, $f(R)$ gravity, $f(\mathcal{T})$ gravity, $f(\mathcal{G})$ gravity, Gauss-Bonnet gravity, Horava-Lifshitz gravity, and Brans-Dicke gravity [30–41]. The $f(R,\nabla R)$ gravity is a theory based on an action integral whose kernel is a function of the Ricci scalar R and terms involving its derivatives. Cuzinatto et al. [42] have explored the cosmological consequences of a particular model in the context of this gravity theory. They tested the model against some of the observational data available. A more recent example is the (nonlocal) higher derivative cosmology presented in [43–46].

Recently the reconstruction procedure or correspondences between various DE models become very challenging subject in cosmological phenomena. The correspondence between different DE models, reconstruction of DE/gravity, and their cosmological implications have been discussed by several authors [47–60]. In the present work, we assume $f(R,\nabla R)$ gravity model in FRW universe. We discuss the correspondence of $f(R,\nabla R)$ gravity with some scalar field dark energy models like quintessence, tachyon, dilaton, k-essence, hessence, and DBI-essence models. The nature of scalar fields and the potentials is analyzed by graphical behavior of their scalar field and potential functions. The scheme of the paper is as follows. In Section 2, we briefly provide a review of $f(R,\nabla R)$ gravity and discuss behavior of EoS and stability parameters. Section 3 devotes the analysis of correspondence between this gravity model and some scalar field models. The last section summarizes the obtained results.

2. Brief Review of $f(R,\nabla R)$ Gravity

The action of $f(R,\nabla R)$ gravity is given by [42]

$$S=\int d^4x\sqrt{-g}\left(\frac{R}{2\kappa^2}+\frac{\beta}{8\kappa^2}\nabla_\mu R\nabla^\mu R-L_m\right), \tag{1}$$

where $\kappa^2=8\pi G=m_p^{-2}$, β is the coupling constant, ∇_μ is the covariant derivative, and L_m is the matter Lagrangian density. An important feature of S is the presence of ghosts [46]. However, here this is not a serious issue because (1) should be considered as an effective action of a fundamental theory of gravity, which make it ghost-free theory. The extended theory of gravity such as String-inspired nonlocal higher derivative gravitational model draws the attention of the researchers. The ghost-free action of this model is given by (the derivation has been discussed in detail by Biswas et al. [45])

$$S=\int d^4x\sqrt{-g}\left(\frac{m_p^2}{2}R+\frac{1}{2}R\mathcal{F}\left(\frac{\Box}{M_*^2}\right)R\right), \tag{2}$$

where M_* denotes the mass scale and term

$$\mathcal{F}\left(\frac{\Box}{M_*^2}\right)=\sum_{n=1}^{\infty}f_n\Box^n. \tag{3}$$

In order to maintain consistency with the action as low energy limiting case, the only suitable contribution of (3) is the first term of the series. That is, the corresponding term is $f_1\gg f_n$, $\forall n\geq 2$. This leads to the equivalence of both actions (1) and (2) up to surface term and yields a relation; that is,

$$f_1=\frac{\beta}{4\kappa^2}. \tag{4}$$

Taking the variation of action (1) with respect to $g_{\mu\nu}$, the field equations turn out to be [42]

$$R_{\mu\nu}-\frac{1}{2}g_{\mu\nu}R+\beta H_{\mu\nu}=\frac{1}{m_p^2}T_{\mu\nu}, \tag{5}$$

where

$$\begin{aligned}H_{\mu\nu}&=\nabla_\mu\nabla_\nu\left[\Box R\right]+\frac{1}{2}\nabla_\mu R\nabla_\nu R-R_{\mu\nu}\Box R\\&\quad-g_{\mu\nu}\Box\left[\Box R\right]-\frac{1}{4}g_{\mu\nu}\nabla_\rho R\nabla^\rho R.\end{aligned} \tag{6}$$

Here $\Box=\nabla_\mu\nabla^\mu$ and $R_{\mu\nu}$ is the Ricci tensor.

For FRW universe, the Friedmann equations in the scenario of $f(R,\nabla R)$ model turn out to be

$$3H^2+\beta F_1=\frac{1}{m_p^2}\rho_m,\qquad 3H^2+2\dot{H}+\beta F_2=-\frac{1}{m_p^2}p_m. \tag{7}$$

Here F_1 and F_2 are defined in terms of Hubble parameter as follows:

$$\begin{aligned}F_1&=18HH^{(4)}+108H^2\dddot{H}-18\dot{H}\dddot{H}+9\ddot{H}^2+90H^3\ddot{H}\\&\quad+216H\dot{H}\ddot{H}-72\dot{H}^3+288\left(H\dot{H}\right)^2-216H^4\dot{H},\\F_2&=6H^{(5)}+54HH^{(4)}+138H^2\dddot{H}+126\dot{H}\dddot{H}+81\ddot{H}^2\\&\quad+18H^3\ddot{H}+498H\dot{H}\ddot{H}+120\dot{H}^3-216H^4\dot{H},\end{aligned} \tag{8}$$

where $H^{(5)}$ denotes the fifth order time derivative of Hubble parameter. The equation of continuity of CDM takes the following form:

$$\dot{\rho}_m+3H\rho_m=0,\quad \text{which gives } \rho_m=\rho_{m0}a^{-3}. \tag{9}$$

The term ρ_{m0} represents the present value of cold matter density. We can extract the EoS parameter; that is, $\omega_R=p_R/\left(\rho_m+\rho_R\right)$, where

$$\rho_R=m_p^2\beta F_1,\qquad p_R=m_p^2\beta F_2. \tag{10}$$

It follows that

$$\omega_R=\frac{m_p^2\beta F_2}{m_p^2\beta F_1+\rho_{m0}a^{-3}}. \tag{11}$$

For the reconstructed scenario, we consider the solution of the field equation in exact power law form given by

$$a(t)=a_0\left(t_s-t\right)^n,\quad t_s>t, \tag{12}$$

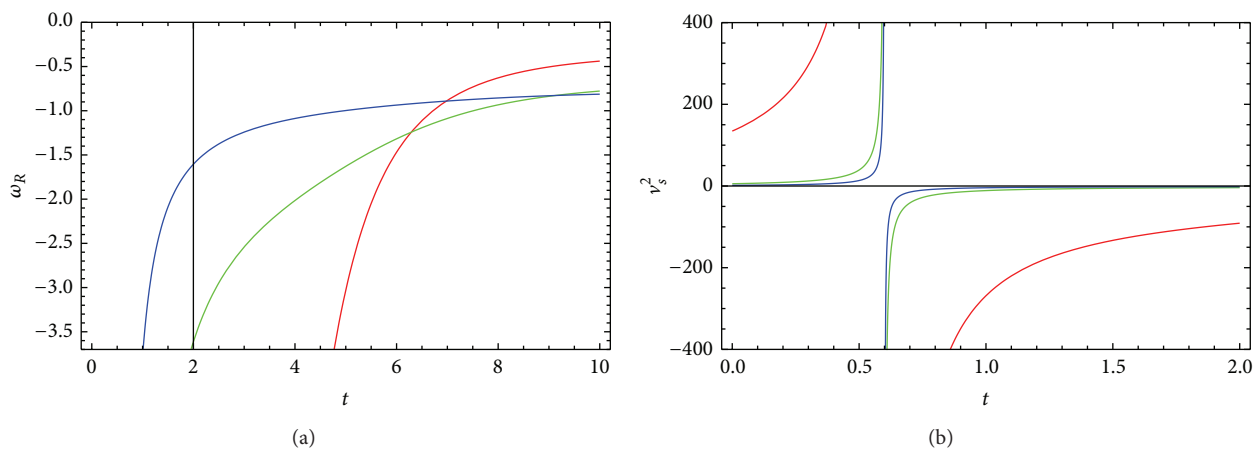

Figure 1: Plots of (a) effective EoS parameter and (b) squared speed of sound versus cosmic time t, for $n = 1$ (red), $n = 2$ (green), and $n = 3$ (blue).

where a_0 is the present value of scale factor and n is a constant. The term t_s denotes the finite future singularity time and the scale factor (12) is used to check type II (sudden singularity) or type IV (corresponds to $\dot{H}$) for positive values of n. We plot effective EoS parameter ω_R versus time as shown in Figure 1(a) for different values of n such that $n = 1, 2, 3$. We choose some typical values of constants in this respect; that is, $\beta = 2.02$, $m_p^2 = 1$, and $t_s = 0.6$. This parameter shows increasing behavior and transition from phantom to quintessence phase. For $n = 1$, ω_R becomes nearly constant at $\omega_R = -0.4$ which represents the quintessence era. As we increase the value of n, this parameter again expresses transition from phantom to quintessence with the passage of time but converges to a value that nearly corresponds to vacuum era of the universe.

To check the stability of the model, we plot squared speed of sound ($v_s^2 = \dot{p}/\dot{\rho}$) versus time as shown in Figure 1(b). The sign of squared speed of sound has a significant role in this regard. A positive value indicates the stability of model whereas instability stands for the negative value of v_s^2. In the plot, we obtain two regions corresponding to the sign as $t < 0.6$ and $t > 0.6$. For the region $t < 0.6$, it is found that v_s^2 represents positively decreasing behavior which gives the stability of the model. In the second region, squared speed of sound represents the instability of the model by experiencing negative behavior for all values of n.

3. Correspondence between $f(R, \nabla R)$ and Scalar Field Models

Here, we investigate the correspondence of $f(R, \nabla R)$ gravity with some of the scalar field models such as quintessence, tachyon, k-essence, dilaton, hessence, and DBI-essence models. The scalar field models have been developed through particle physics as well as string theory and nowadays these are used as a DE candidate.

3.1. Quintessence. The quintessence scalar field model has been proposed to resolve the fine-tuning problem taking EoS as time dependent instead of constant. This model can explain current cosmic acceleration by giving negative pressure when potential dominates the kinetic term. It is minimally coupled with gravity and used as a useful tool for discussing early inflation as well as the late time acceleration. The action of this model is described as [14–16]

$$S_Q = \int d^4x \sqrt{-g} \left[-\frac{1}{2} (\nabla\phi)^2 - V(\phi) \right], \tag{13}$$

where $(\nabla\phi)^2 = g^{\mu\nu}\partial_\mu\phi\partial_\nu\phi$ and $V(\phi)$ denotes the potential of the field. Varying this action with respect to metric tensor $g^{\mu\nu}$, we obtain the corresponding energy-momentum tensor as follows:

$$T_{\mu\nu} = \partial_\mu\phi\partial_\nu\phi - g_{\mu\nu} \left[\frac{1}{2} g^{\alpha\beta}\partial_\alpha\phi\partial_\beta\phi + V(\phi) \right]. \tag{14}$$

This gives the energy density and pressure for FRW universe as follows:

$$\rho_Q = -T_0^0 = \frac{1}{2}\dot{\phi}^2 + V(\phi), \qquad p_Q = T_i^i = \frac{1}{2}\dot{\phi}^2 - V(\phi). \tag{15}$$

These expressions yield

$$\dot{\phi}^2 = \rho_Q + p_Q, \qquad V(\phi) = \frac{1}{2}(\rho_Q - p_Q). \tag{16}$$

Replacing ρ_Q and p_Q by the energy density and pressure of $f(R, \nabla R)$ model, we study the behavior of the resulting scalar field and potential function.

The evolution trajectories of scalar field and potential function versus time for $f(R, \nabla R)$ quintessence model are shown in Figure 2 taking the same values of constants as for effective EoS parameter. In left plot (a), $\phi(t)$ represents increasing behavior and becomes more steeper as time goes

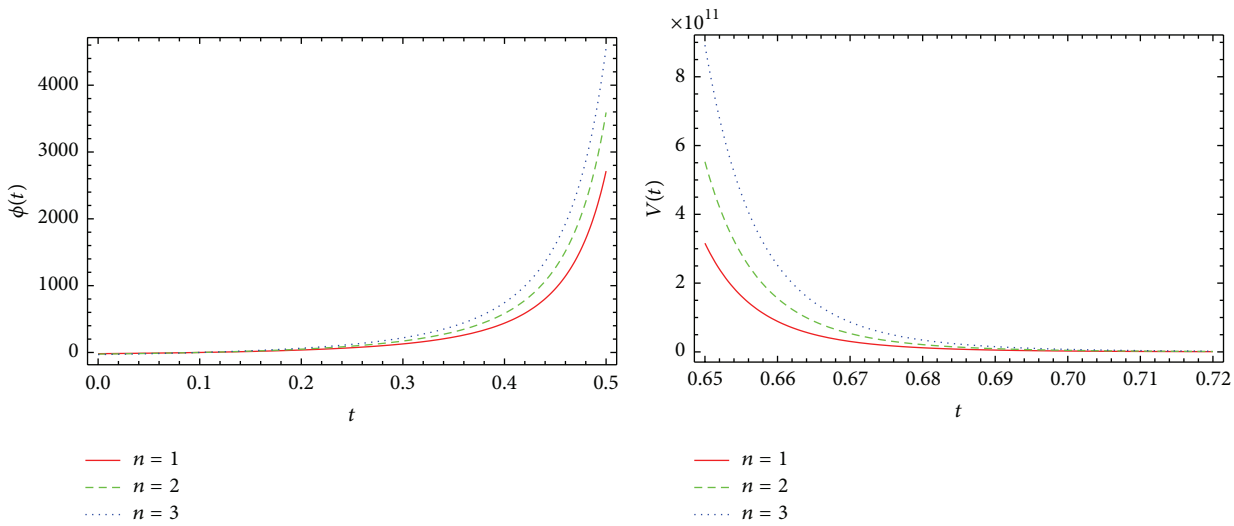

(a) Scalar field $\phi(t)$

(b) Potential function $V(t)$

FIGURE 2: Plots of $f(R, \nabla R)$ quintessence scalar field model: (a) scalar field ϕ and (b) potential V versus cosmic time t.

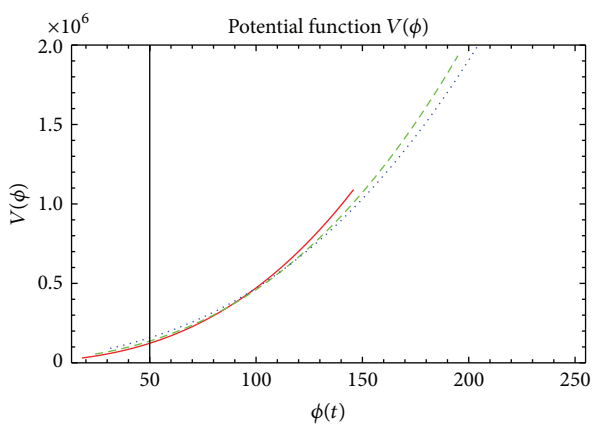

FIGURE 3: Plot of $f(R, \nabla R)$ quintessence potential V versus $\phi(t)$ for $n = 1$ (red), $n = 2$ (green), and $n = 3$ (blue).

on, particularly for greater value of n. The increasing value of scalar field indicates that kinetic energy is decreasing. The potential function versus time in plot (b) expresses decreasing behavior. The plot of quintessence potential in terms of scalar field is shown in Figure 3 representing increasing behavior. The gradually decreasing kinetic energy while potential remains positive for $f(R, \nabla R)$ quintessence model represents accelerated expansion of the universe.

3.2. Tachyon. The tachyon model is motivated from string theory and used as a possible candidate to explain DE scenario. It is argued that rolling tachyon condensates possess useful cosmological consequences. The EoS of this rolling tachyon is smoothly interpolated between -1 and 0 which is an interesting feature of this model. This has led a flurry of attempts to construct more viable cosmological models for tachyon which serves as a suitable candidate of inflation at high energy. It is realized that tachyon can be used as a source of DE depending on different forms of its potential. The effective Lagrangian for tachyon is [11, 14]

$$S_T = -\int d^4x V(\phi) \sqrt{-\det\left(g_{\mu\nu} + \partial_\mu\phi\partial_\nu\phi\right)}. \tag{17}$$

Varying this action with respect to the metric tensor, we have

$$T_{\mu\nu} = \frac{V(\phi)\,\partial_\mu\phi\partial_\nu\phi}{\sqrt{1 + g^{\alpha\beta}\partial_\alpha\phi\partial_\beta\phi}} - g_{\mu\nu}V(\phi)\sqrt{1 + g^{\alpha\beta}\partial_\alpha\phi\partial_\beta\phi}, \tag{18}$$

leading to the energy density and pressure as

$$\rho_T = \frac{V(\phi)}{\sqrt{1 - \dot{\phi}^2}}, \qquad p_T = -V(\phi)\sqrt{1 - \dot{\phi}^2}, \tag{19}$$

and EoS parameter becomes

$$\omega_T = \dot{\phi}^2 - 1. \tag{20}$$

Taking into account (19) and (20), we have

$$\dot{\phi}^2 = 1 + \omega_T, \qquad V(\phi) = \rho_T\sqrt{\omega_T}, \tag{21}$$

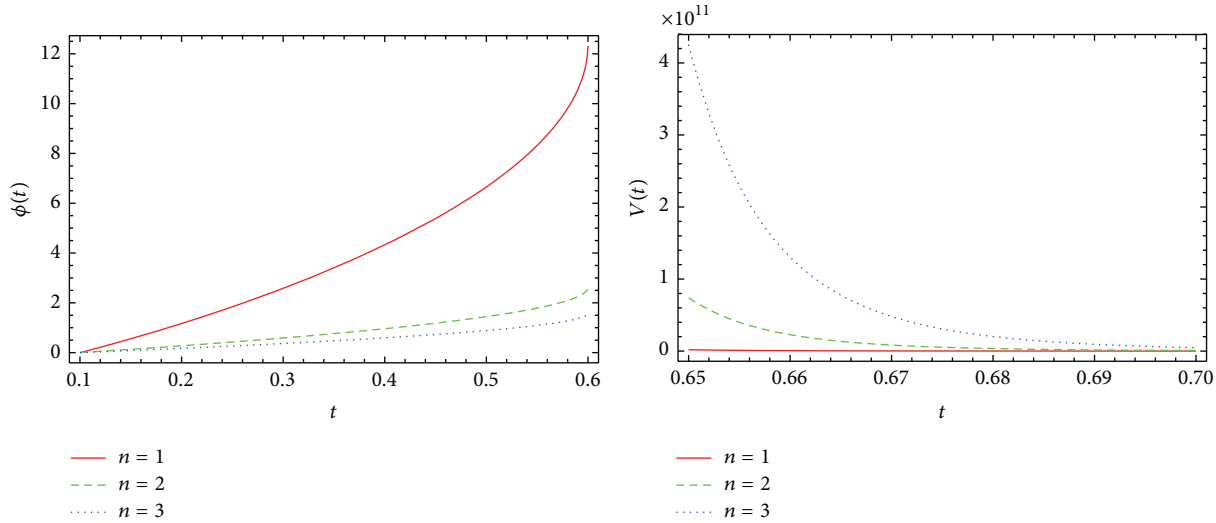

(a) Scalar field $\phi(t)$

(b) Potential function $V(t)$

FIGURE 4: Plots of $f(R, \nabla R)$ tachyon model: (a) scalar field ϕ versus time t and (b) potential V versus time t for $n = 1$ (red), $n = 2$ (green), and $n = 3$ (blue).

which can be replaced by ρ_R and ω_R in order to check the behavior of scalar field and potential function of $f(R, \nabla R)$ tachyon model.

We plot scalar field and potential function of $f(R, \nabla R)$ tachyon model as shown in Figure 4. The evolution of this model is much similar to the quintessence model. The scalar field represents increasing behavior versus time and indicates more steeper behavior for $n = 1$. This leads to the decreasing kinetic energy, approximately zero value. This represents the vacuum behavior of the universe depicted by (20). The corresponding potential function expresses decreasing but positive behavior with respect to t. Its decreasing behavior from maxima gives inverse proportionality to the scalar field for the later times. This type of behavior corresponds to scaling solutions in the brane-world cosmology [61, 62].

3.3. k-Essence. Armendáriz-Picón et al. [63] introduced the concept inflation driven by kinetic energy (termed as k-inflation) for discussing the inflation in the early universe at high energies. This scenario was used for DE purpose by Chiba et al. [64]. Moreover, this analysis was extended by Armendáriz-Picón et al. [65] to a more generalized form of Lagrangian, named as "k-essence." The quintessence scalar field relies on potential energy in order to explain late time cosmic acceleration of the universe. However, this model takes the modifications of kinetic energy in the scalar fields to address the cosmic expansion. The generalized form of scalar field action is

$$S_K = \int d^4x \sqrt{-g} p(\phi, \chi), \tag{22}$$

where $p(\phi, \chi)$ shows the pressure density as a function of potential ϕ and $\chi = (1/2)\dot{\phi}^2$. The energy density and pressure are given by

$$\rho_K = V(\phi)\left(-\chi + 3\chi^2\right), \qquad p_K = V(\phi)\left(-\chi + \chi^2\right). \tag{23}$$

The corresponding EoS parameter yields

$$\omega_K = \frac{1-\chi}{1-3\chi}, \tag{24}$$

which represents the fact that the accelerated expansion of the universe is experienced for the interval $(1/3, 2/3)$ for χ. The potential function takes the form

$$V(\phi) = \frac{(1-3\omega_K)^2}{2(1-\omega_K)}\rho_K. \tag{25}$$

Equating $\omega_K = \omega_R$ and $\rho_K = \rho_R$ in (24) and (25), the evolution trajectories of ϕ and χ versus t for $f(R, \nabla R)$ k-essence scalar field model are given in Figure 5. The plot (a) represents increasing behavior of scalar field with respect to time for all values of n. The plot (b) of χ versus t shows compatible behavior of the model for all n from early era to later times. This indicates that for $t \geq 0.6$, $\chi(t)$ approaches to the required interval for accelerated expansion of the universe. Also, the potential function versus t and ϕ is shown in Figures 6(a)-6(b), expressing positively decreasing behavior.

3.4. Dilaton. It is shown [14] that phantom field with negative kinetic energy plagued a problem of quantum instabilities. To avoid this problem, dilaton model has been originated which

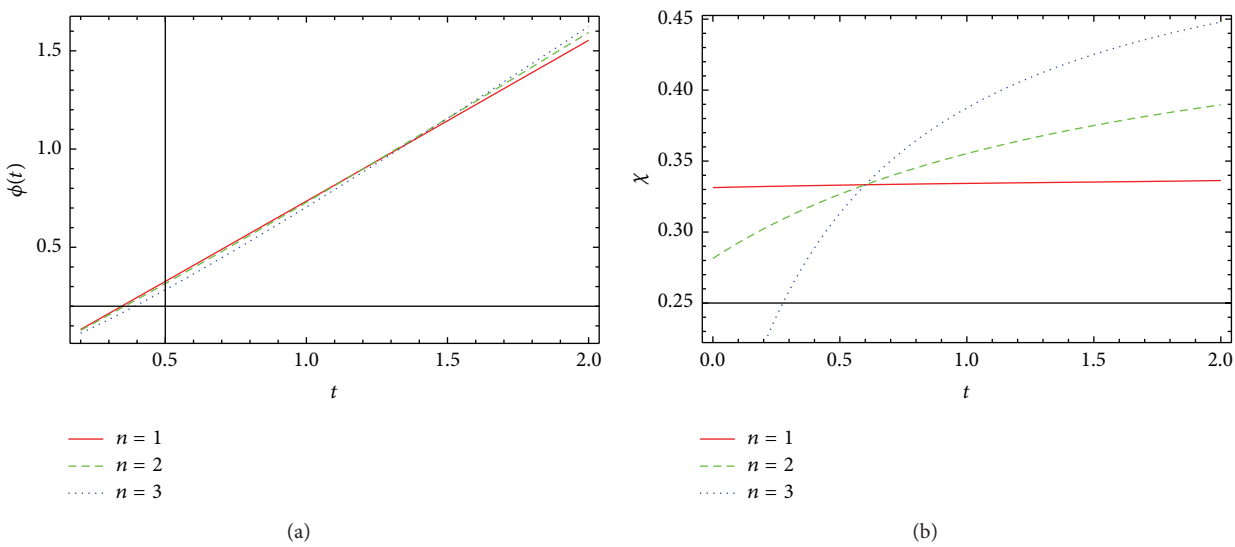

FIGURE 5: Plots of $f(R, \nabla R)$ k-essence scalar field: (a) ϕ versus cosmic time t and (b) kinetic energy term χ versus t for $n = 1$ (red), $n = 2$ (green), and $n = 3$ (blue).

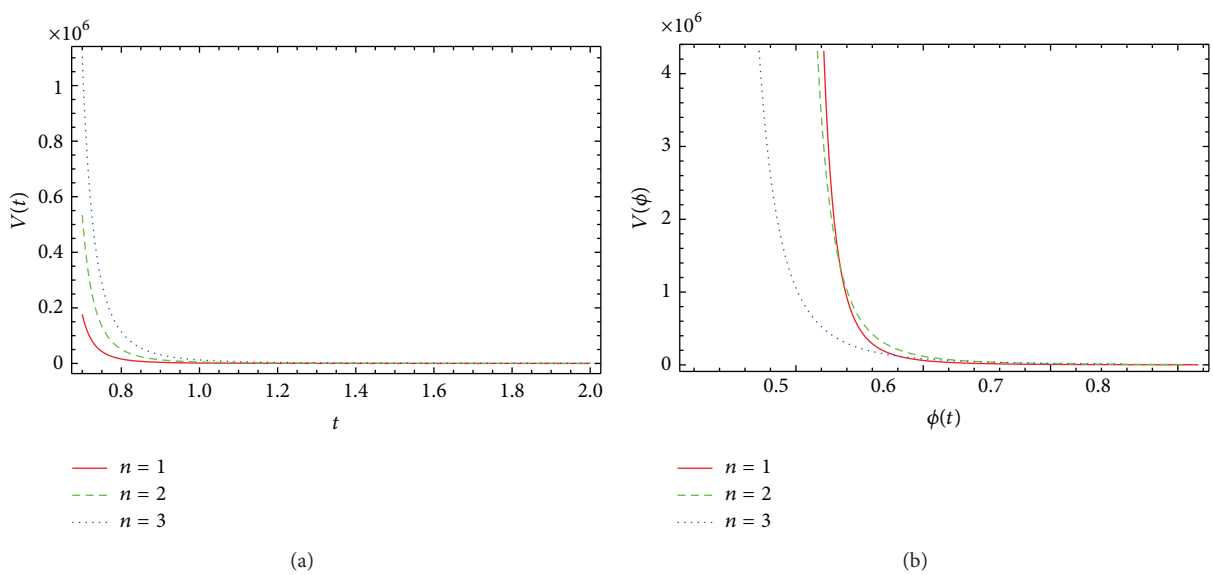

FIGURE 6: Plots of $f(R, \nabla R)$ k-essence potential (a) V versus cosmic time t and (b) V versus ϕ for $n = 1$ (red), $n = 2$ (green), and $n = 3$ (blue).

is later used to explain DE puzzle. Also, it is realized that this model avoids some quantum instabilities with respect to the phantom field models of DE. This model is found in low energy effective string theory, where dilatonic higher-order corrections were made to the tree-level action. The Lagrangian of dilaton field can be expressed in terms of pressure of scalar field as [14, 18]

$$p_D = -\chi + c_1 e^{b\phi} \chi^2, \tag{26}$$

where c_1 and c_2 are taken to be positive constants. This Lagrangian (pressure) produces the following energy density:

$$\rho_D = -\chi + 3c_1 e^{b\phi} \chi^2. \tag{27}$$

The EoS parameter takes the form

$$\omega_D = \frac{1 - c_1 e^{b\phi} \chi}{1 - 3c_1 e^{b\phi} \chi}. \tag{28}$$

By keeping $\rho_D = \rho_R$ and $p_D = p_R$ in above three equations, we can get kintetic energy corresponding scalar

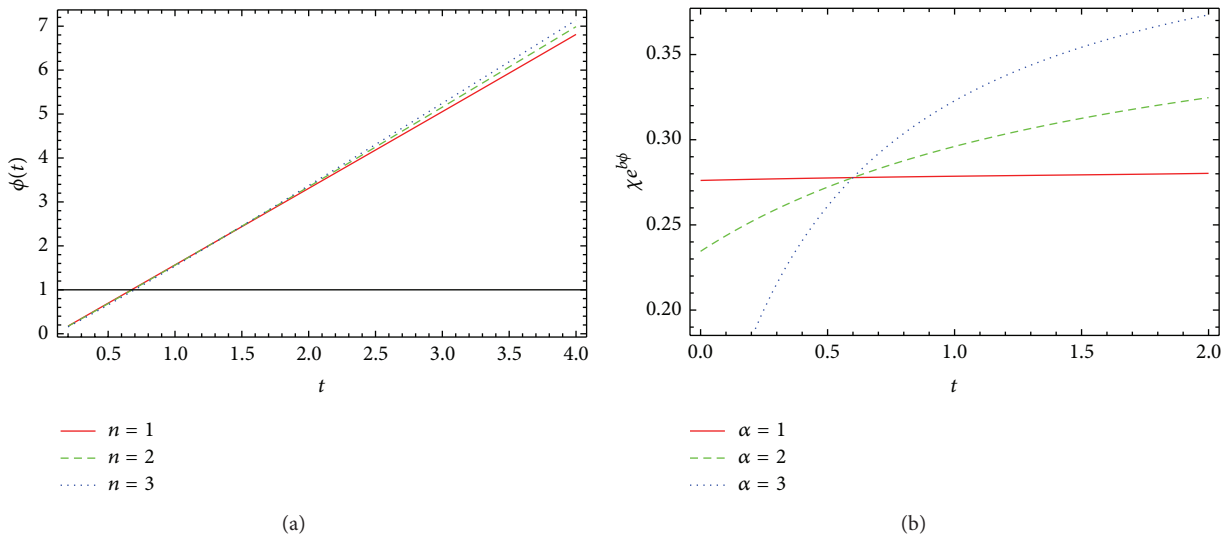

Figure 7: Plots of $f(R, \nabla R)$ dilaton scalar field model (a) ϕ versus cosmic time t and (b) kinetic energy term $\chi e^{b\phi}$ versus t for $n = 1$ (red), $n = 2$ (green), and $n = 3$ (blue).

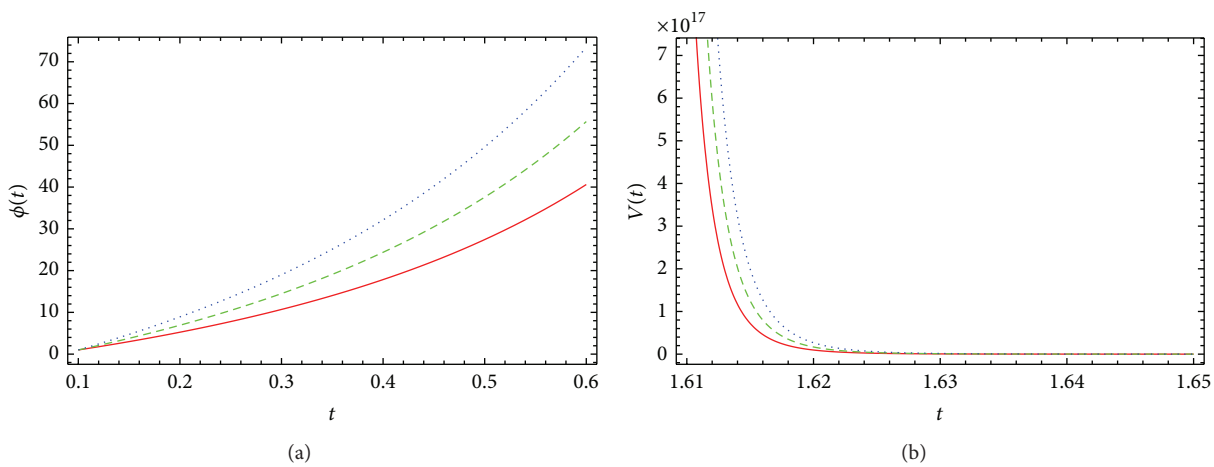

Figure 8: Plots of $f(R, \nabla R)$ hessence scalar field model: (a) ϕ versus cosmic time t and (b) potential V versus t for $n = 1$ (red), $n = 2$ (green), and $n = 3$ (blue).

field numerically by keeping same values for other constants while $c_1 = 1.2$. The behavior of this model is approximately the same as of the k-essence model. Figure 7(a) represents the increasing behavior of scalar field versus time. In plot (b), the kinetic energy term $\chi e^{b\phi}$ versus time shows increasing behavior with the passage of time. The EoS parameter given in (28) indicates the bound of kinetic energy term such as $(5/18, 5/9)$ for accelerated expansion of the universe. In this regard, we observe that the value $n = 1$ is inconsistent with this interval while the remaining values of n represent compatible results.

3.5. Hessence. The noncanonical complex scalar field, $\Phi = \phi_1 + \imath\phi_2$ named as hessence, has the Lagrangian density as [21]

$$L_H = \frac{1}{2}\left[\left(\partial_\mu\phi\right)^2 - \phi^2\left(\partial_\mu\phi\right)^2\right] - V(\phi), \tag{29}$$

where $\phi = \phi_1^2 + \phi_2^2$ with $\phi_1 = \phi\cosh\theta$ and $\phi_2 = \phi\sinh\theta$ which lead to $\coth\theta = \phi_1/\phi_2$. These two variables (ϕ, θ) are introduced to describe the hessence scalar field. The hessence comprises the special case of quintom model in terms of ϕ_1 and ϕ_2. For FRW spacetime, the energy density and pressure take the form

$$\begin{aligned} p_H &= \frac{1}{2}\left[\dot{\phi}^2 - \frac{Q^2}{a^6\phi^2}\right] - V(\phi), \\ \rho_H &= \frac{1}{2}\left[\dot{\phi}^2 - \frac{Q^2}{a^6\phi^2}\right] + V(\phi), \end{aligned} \tag{30}$$

where Q represents the total conserved charge within the physical volume due to the internal symmetry. Using (30), we

obtain the scalar field and potential of hessence scalar filed model as

$$\dot{\phi}^2 - Q^2 a^{-6}\phi^{-2} = \rho_H - p_H, \qquad V(\phi) = \frac{1}{2}(\rho_H - p_H). \tag{31}$$

Replacing energy density and potential of hessence scalar field with ρ_R and p_R in the above equations, we plot scalar field and potential of $f(R,\nabla R)$ hessence scalar field model as shown in Figure 8. The scalar field ϕ expresses increasing behavior with respect to t as shown in plot (a). In plot (b), the potential function represents the same behavior as the remaining scalar field models. Initially, this indicates decreasing behavior with the passage of time.

3.6. DBI-Essence. Here we consider Dirac-Born-Infeld-(DBI-) essence scalar field model whose action is given by [19, 20]

$$S_{\text{dbi}} = \int d^4x a^3(t)\left[T(\phi)\sqrt{1-\frac{\dot{\phi}^2}{T(\phi)}} + V(\phi) - T(\phi)\right], \tag{32}$$

where $T(\phi)$ and $V(\phi)$ are the warped brane tension and the DBI potential, respectively. The corresponding energy density and pressure yield

$$\begin{aligned}\rho_{\text{dbi}} &= (\gamma-1)T(\phi) + V(\phi),\\ p_{\text{dbi}} &= \left(1-\frac{1}{\gamma}\right)T(\phi) - V(\phi),\end{aligned} \tag{33}$$

where $\gamma = \left(1-\left(\dot{\phi}^2/T(\phi)\right)\right)^{-1/2}$ is reminiscent from the usual relativistic Lorentz factor. Now, we consider here two particular cases which involve γ as a constant and vice versa.

Case 1 (γ = constant). In this case, we assume γ as constant and $T(\phi) = m\dot{\phi}^{-2}$ where $m > 1$ for the sake of simplicity. The γ becomes

$$\gamma = \sqrt{\frac{m}{m-1}}. \tag{34}$$

Using (33), we obtain the following expressions for DBI-essence for constant γ:

$$\dot{\phi}^2 = \frac{\gamma}{m(\gamma^2-1)}(\rho_{\text{dbi}} + p_{\text{dbi}}), \tag{35}$$

$$V(\phi) = \frac{1}{2}\left[(\rho_{\text{dbi}} - p_{\text{dbi}}) - \left(\gamma - 2 + \frac{1}{\gamma}\right)T(\phi)\right], \tag{36}$$

where $T(\phi) = \left(\gamma/(\gamma^2-1)\right)(\rho_{\text{dbi}} + p_{\text{dbi}})$. Inserting energy density and pressure of $f(R,\nabla R)$ model with those of ρ_{dbi} and p_{dbi} in (35), we plot ϕ and V versus t as shown in Figure 9. This represents approximately the same behavior as for $f(R,\nabla R)$ quintessence scalar field model. The scalar field shows increasing behavior while potential represents decreasing but positive behavior.

Case 2 ($\gamma \neq$ constant). Here we take γ not as a constant. For this purpose, we assume $\gamma = \dot{\phi}^s$ where s is an arbitrary constant. This case leads to the following expressions:

$$\begin{aligned}\dot{\phi} &= (\rho_{\text{dbi}} + p_{\text{dbi}})^{1/(s+2)},\\ V(\phi) &= \frac{1}{2}\left[(\rho_{\text{dbi}} - p_{\text{dbi}}) - \left(\gamma - 2 + \frac{1}{\gamma}\right)T(\phi)\right],\end{aligned} \tag{37}$$

where $T(\phi) = \dot{\phi}^{2s+2}/(\dot{\phi}^{2s} - 1)$. In order to plot scalar field and potential of $f(R,\nabla R)$ DBI-essence scalar field (with $\gamma \neq$ constant), we substitute $\rho_{\text{dbi}} = \rho_R$ and $p_{\text{dbi}} = p_R$ in (37). Figure 10 represents the same behavior as for constant γ; however, the values of scalar field and potential are quite different in both cases.

4. Concluding Remarks

In this work, we have discussed the flat FRW universe model in the framework of $f(R,\nabla R)$ gravity. We have obtained the modified Friedmann equations and the effective energy density as well as pressure coming from extra terms of the $f(R,\nabla R)$ gravity sector. These can be treated as DE provided that the strong energy condition violates. We have assumed the power law solution of scale factor $a(t) = a_0(t_s - t)^n$, $t_s > t$. The term t_s denotes the finite future singularity time and the scale factor is used to check type II (sudden singularity) or type IV (corresponds to $\dot{H}$) for positive values of n. We have plotted the effective EoS parameter ω_R versus time in Figure 1(a) for different values of $n = 1, 2, 3$ and $\beta = 2.02$, $m_p^2 = 1$, and $t_s = 0.6$. The EoS parameter shows increasing nature and transition from phantom to quintessence phase. For $n = 1$, the ω_R becomes nearly constant at $\omega_R = -0.4$ which represents the quintessence era. For increasing values of n, the EoS parameter again expresses transition from phantom to quintessence in the course of time, but this converges to vacuum era of the universe. In Figure 1(b), we have plotted squared speed of sound v_s^2 versus time. A positive value indicates the stability of model whereas instability stands for the negative value of v_s^2. We obtain two regions corresponding to the sign as $t < 0.6$ and $t > 0.6$. For the region $t < 0.6$, it is found that squared speed of sound represents positively decreasing behavior which gives the stability of the model for all values of n. In the second region, squared speed of sound represents negative behavior which gives the instability (classically unstable) of the model for all values of n.

Since scalar field models of DE are effective theories of an underlying theory of DE, we have studied the correspondence between the effective DE coming from $f(R,\nabla R)$ gravity with other scalar field DE models like quintessence, tachyon, k-essence, dilaton, hessence, and DBI-essence and constructed the scalar field as well as corresponding scalar potentials which describe the dynamics of the scalar fields graphically. We have taken the same values of the parameters in all cases taking different values of power of scale factor. The physical interpretations of all the DE models are summarized as follows.

The evolution trajectories of scalar field and potential function versus time for the correspondence of $f(R,\nabla R)$

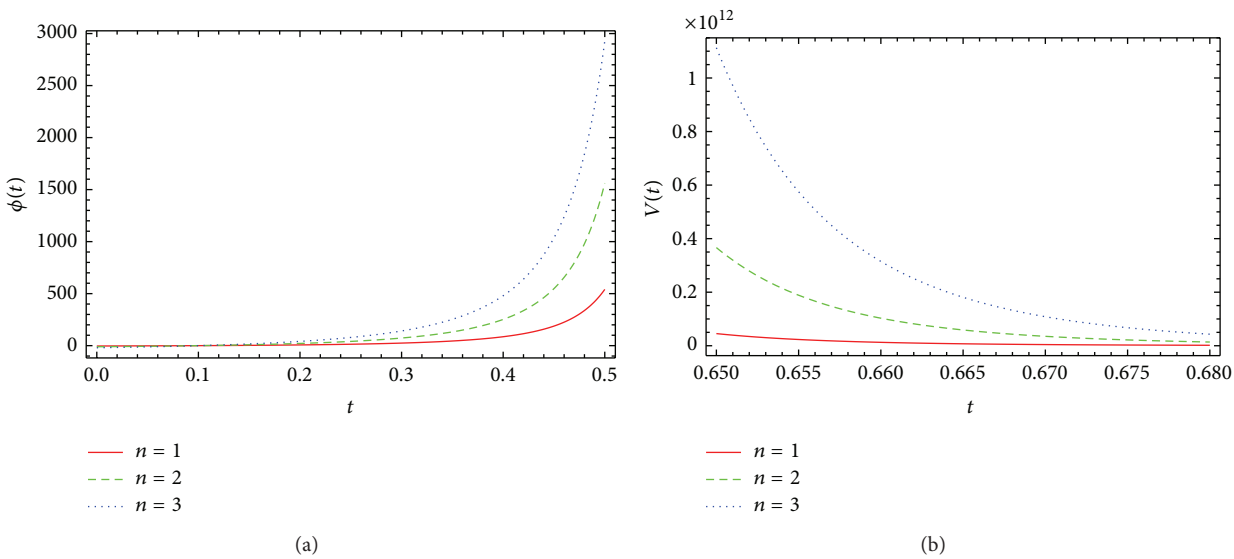

FIGURE 9: Plots of $f(R, \nabla R)$ DBI-essence scalar field (with constant γ): (a) ϕ versus cosmic time t and (b) potential versus t for $n = 1$ (red), $n = 2$ (green), and $n = 3$ (blue).

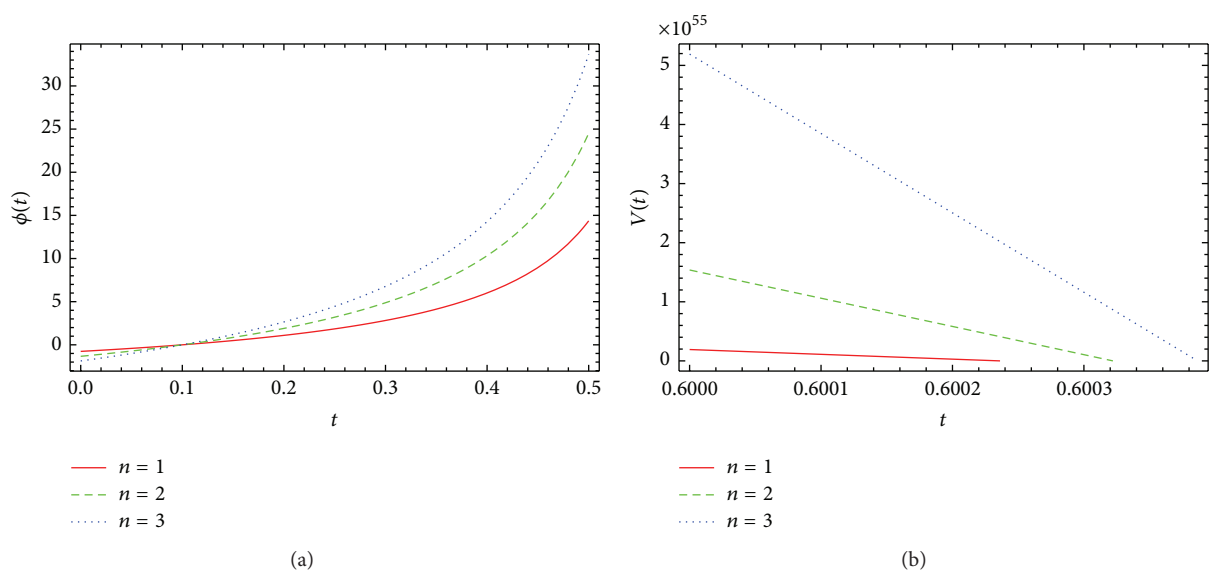

FIGURE 10: Plots of $f(R, \nabla R)$ DBI-essence scalar field (with $\gamma \neq$ constant): (a) ϕ versus cosmic time t and (b) potential versus t (right panel) for $n = 1$ (red), $n = 2$ (green), and $n = 3$ (blue).

with *quintessence dark energy model* are shown in Figure 2 by taking the same values of constants as for effective EoS parameter ω_R. From Figure 2(a), we have observed that the quintessence scalar field $\phi(t)$ represents increasing behavior and becomes more steeper as time goes on, particularly for greater value of n. The increasing value of scalar field indicates that kinetic energy is decreasing. The potential function versus time in plot 2(b) expresses decreasing nature. The plot of quintessence potential in terms of scalar field is shown in Figure 3 representing increasing behavior. The gradually decreasing kinetic energy while potential remains positive for quintessence model represents accelerated expansion of the universe.

We have plotted the scalar field and potential function of *tachyon model* in Figure 4 for the correspondence scenario. The scalar field (Figure 4(a)) represents increasing behavior versus time and indicates more steeper behavior for $n = 1$. This leads to the positively decreasing kinetic energy, which approximately tends to zero (i.e., the vacuum). The corresponding potential function (Figure 4(b)) expresses decreasing but positive behavior with respect to t. Its decreasing behavior from maxima gives inverse proportionality to the scalar field for the later times. This type of behavior corresponds to scaling solutions in the brane-world cosmology.

The *k-essence model* expresses the evolution of scalar field and kinetic energy term versus t. The evolution trajectories of

ϕ and χ versus t for $f(R, \nabla R)$ k-essence scalar field model are given in Figure 5. The plot 5(a) represents increasing behavior of scalar field with respect to time for all values of n. The plot 5(b) of χ versus t shows compatible behavior of the model for all n from early era to later times. This indicates that, for $t \geq 0.6$, $\chi(t)$ approaches to the required interval for accelerated expansion of the universe. Also, the potential function versus t and ϕ is shown in Figures 6(a)-6(b), expressing positively decreasing nature.

The scalar field and kinetic energy term of *dilaton model* are drawn in Figure 7, keeping the same values for other constants while $c_1 = 1.2$. Figure 7(a) represents the increasing behavior of scalar field versus time. In the plot 7(b), the kinetic energy term $\chi e^{b\phi}$ versus time shows increasing behavior in the course of time. The EoS parameter indicates the bound of kinetic energy term such as $(5/18, 5/9)$ for accelerated expansion of the universe. In this regard, we observe that the value $n = 1$ is inconsistent with this interval while the remaining values of n represent compatible results.

For *hessence model*, scalar field and potential are shown in Figure 8. The scalar field expresses increasing behavior with respect to t, which is shown in Figure 8(a). In plot 8(b), the potential function represents the same behavior as the remaining scalar field models. Initially, this indicates decreasing behavior with the passage of time. It is noted that if $Q = 0$, the hessence model may generate the scalar field model for quintessence. So quintessence model is the special case of hessence model.

We have studied scalar field and potential functions of *DBI-essence model* taking constant and variable DBI-parameter, which have been drawn in Figures 9 and 10. The scalar field shows increasing behavior while potential represents decreasing but positive behavior in both cases.

Conflict of Interests

The authors declare that there is no conflict of interests regarding the publication of this paper.

References

[1] S. Perlmutter, G. Aldering, M. D. Valle et al., "Discovery of a supernova explosion at half the age of the universe," *Nature*, vol. 391, no. 6662, pp. 51–54, 1998.

[2] A. G. Riess, A. V. Filippenko, and P. Challis, "Observational evidence from supernovae for an accelerating universe and a cosmological constant," *The Astronomical Journal*, vol. 116, p. 1009, 1998.

[3] M. Tegmark, M. Strauss, M. Blanton et al., "Cosmological parameters from SDSS and WMAP," *Physical Review D*, vol. 69, Article ID 103501, 2004.

[4] D. N. Spergel, L. Verde, H. V. Peiris et al., "First year *Wilkinson Microwave Anisotropy Probe (WMAP)* observations: determination of cosmological parameters," *The Astrophysical Journal Supplement*, vol. 148, no. 1, pp. 175–194, 2003.

[5] S. Briddle, O. Lahav, J. P. Ostriker, and P. J. Steinhardt, "Precision cosmology? Not just yet," *Science*, vol. 299, pp. 1532–1533, 2003.

[6] A. Einstein, *Sitzungsberichte der Preussischen Akademie der Wissenschaften*, vol. 1917, p. 142, 1917.

[7] S. Weinberg, "The cosmological constant problem," *Reviews of Modern Physics*, vol. 61, no. 1, pp. 1–23, 1989.

[8] V. Sahni and A. Starobinsky, "The case for a postive cosmological λ-term," *International Journal of Modern Physics D*, vol. 9, no. 4, pp. 373–443, 2000.

[9] P. J. Steinhardt, "Cosmological challenges for the 21st century," in *Critical Problems in Physics*, V. L. Fitch and D. R. Marlow, Eds., pp. 123–145, Princeton University Press, 1997.

[10] C. Armendariz-Picon, V. Mukhanov, and P. J. Steinhardt, "Dynamical solution to the problem of a small cosmological constant and late-time cosmic acceleration," *Physical Review Letters*, vol. 85, no. 21, pp. 4438–4441, 2000.

[11] A. Sen, "Tachyon matter," *Journal of High Energy Physics*, vol. 2002, no. 7, article 065, 2002.

[12] B. Feng, X. L. Wang, and X. M. Zhang, "Dark energy constraints from the cosmic age and supernova," *Physics Letters B*, vol. 607, no. 1-2, pp. 35–41, 2005.

[13] A. Kamenshchik, U. Moschella, and V. Pasquier, "An alternative to quintessence," *Physics Letters, Section B: Nuclear, Elementary Particle and High-Energy Physics*, vol. 511, no. 2–4, pp. 265–268, 2001.

[14] E. J. Copeland, M. Sami, and S. Tsujikawa, "Dynamics of dark energy," *International Journal of Modern Physics D*, vol. 15, no. 11, pp. 1753–1935, 2006.

[15] P. J. E. Peebles and B. Ratra, "Cosmology with a time-variable cosmological "constant"," *The Astrophysical Journal*, vol. 325, pp. L17–L20, 1988.

[16] R. R. Caldwell, R. Dave, and P. J. Steinhardt, "Cosmological imprint of an energy component with general equation of state," *Physical Review Letters*, vol. 80, no. 8, pp. 1582–1585, 1998.

[17] A. R. Liddle and R. J. Scherrer, "Classification of scalar field potentials with cosmological scaling solutions," *Physical Review D*, vol. 59, no. 2, Article ID 023509, 7 pages, 1998.

[18] M. Gasperini, F. Piazza, and G. Veneziano, "Quintessence as a runaway dilaton," *Physical Review D*, vol. 65, no. 2, Article ID 023508, 13 pages, 2002.

[19] B. Gumjudpai and J. Ward, "Generalized DBI quintessence," *Physical Review D*, vol. 80, Article ID 023528, 2009.

[20] J. Martin and M. Yamaguchi, "DBI-essence," *Physical Review D*, vol. 77, Article ID 123508, 2008.

[21] H. Wei, R.-G. Cai, and D.-F. Zeng, "Hessence: a new view of quintom dark energy," *Classical and Quantum Gravity*, vol. 22, no. 16, pp. 3189–3202, 2005.

[22] R. R. Caldwell, "A phantom menace? Cosmological consequences of a dark energy component with super-negative equation of state," *Physics Letters B*, vol. 545, no. 1-2, pp. 23–29, 2002.

[23] N. Arkani-Hamed, H.-C. Cheng, M. A. Luty, and S. Mukohyama, "Ghost condensation and a consistent infrared modification of gravity," *Journal of High Energy Physics*, vol. 2004, no. 5, article 074, 2004.

[24] F. Piazza and S. Tsujikawa, "Dilatonic ghost condensate as dark energy," *Journal of Cosmology and Astroparticle Physics*, vol. 2004, no. 7, article 4, 2004.

[25] Z. K. Guo, Y. S. Piao, X. M. Zhang, and Y. Z. Zhang, "Cosmological evolution of a quintom model of dark energy," *Physics Letters B*, vol. 608, pp. 177–182, 2005.

[26] Y. F. Cai, E. N. Saridakis, M. R. Setare, and J. Q. Xia, "Quintom cosmology: theoretical implications and observations," *Physics Reports*, vol. 493, no. 1, pp. 1–60, 2010.

[27] L. Amendola, "Coupled quintessence," *Physical Review D*, vol. 62, no. 4, Article ID 043511, 10 pages, 2000.

[28] X. Zhang, "Coupled quintessence in a power-law case and the cosmic coincidence problem," *Modern Physics Letters A*, vol. 20, no. 33, p. 2575, 2005.

[29] V. Sahni and Y. Shtanov, "Braneworld models of dark energy," *Journal of Cosmology and Astroparticle Physics*, vol. 11, article 014, 2003.

[30] G. Dvali, G. Gabadadze, and M. Porrati, "Metastable gravitons and infinite volume extra dimensions," *Physics Letters B*, vol. 484, no. 1-2, pp. 112–118, 2000.

[31] A. de Felice and T. Tsujikawa, "f(R) theories," vol. 13, article 3, 2010.

[32] M. C. B. Abdalla, S. Nojiri, and S. D. Odintsov, "Consistent modified gravity: dark energy, acceleration and the absence of cosmic doomsday," *Classical and Quantum Gravity*, vol. 22, no. 5, pp. L35–L42, 2005.

[33] E. V. Linder, "Einstein's other gravity and the acceleration of the Universe," *Physical Review D*, vol. 81, Article ID 127301, 2010.

[34] M. Sharif and S. Rani, "Generalized teleparallel gravity via some scalar field dark energy models," *Astrophysics and Space Science*, vol. 345, no. 1, pp. 217–223, 2013.

[35] M. Sharif and S. Rani, "Nonlinear electrodynamics in $f(T)$ gravity and generalized second law of thermodynamics," *Astrophysics and Space Science*, vol. 346, no. 2, pp. 573–582, 2013.

[36] M. Sharif and S. Rani, "Dynamical instability of spherical collapse in $f(T)$ gravity," *Monthly Notices of the Royal Astronomical Society*, vol. 440, no. 3, pp. 2255–2264, 2014.

[37] K. K. Yerzhanov, S. R. Myrzakul, I. I. Kulnazarov, and R. Myrzakulov, "Accelerating cosmology in F(T) gravity with scalar field," http://arxiv.org/abs/1006.3879.

[38] S. Nojiri and S. D. Odintsov, "Modified Gauss-Bonnet theory as gravitational alternative for dark energy," *Physics Letters B*, vol. 631, no. 1-2, pp. 1–6, 2005.

[39] I. Antoniadis, J. Rizos, and K. Tamvakis, "Singularity-free cosmological solutions of the superstring effective action," *Nuclear Physics B*, vol. 415, no. 2, pp. 497–514, 1994.

[40] P. Hořava, "Membranes at quantum criticality," *Journal of High Energy Physics*, vol. 2009, article 020, 2009.

[41] C. Brans and H. Dicke, "Mach's principle and a relativistic theory of gravitation," *Physical Review*, vol. 124, no. 3, pp. 925–935, 1961.

[42] R. R. Cuzinatto, C. A. M. de Melo, L. G. Medeiros, and P. J. Pompeia, "Observational constraints to a phenomenological $f(R, \nabla R)$-model," http://arxiv.org/abs/1311.7312.

[43] S. Gottlober, H.-J. Schmidt, and A. A. Starobinsky, "Sixth-order gravity and conformal transformations," *Classical and Quantum Gravity*, vol. 7, no. 5, pp. 893–900, 1990.

[44] T. Biswas, A. Mazumdar, and W. Siegel, "Bouncing universes in string-inspired gravity," *Journal of Cosmology and Astroparticle Physics*, vol. 2006, no. 3, article 009, 2006.

[45] T. Biswas, T. Koivisto, and A. Mazumdar, "Towards a resolution of the cosmological singularity in non-local higher derivative theories of gravity," *Journal of Cosmology and Astroparticle Physics*, vol. 2010, article 008, 2010.

[46] T. Biswas, A. S. Koshelev, A. Mazumdar, and S. Y. Vernov, "Stable bounce and inflation in non-local higher derivative cosmology," *Journal of Cosmology and Astroparticle Physics*, vol. 2012, no. 8, article 024, 2012.

[47] K. Karami and M. S. Khaledian, "Reconstructing $f(R)$ modified gravity from ordinary and entropy-corrected versions of the holographic and new agegraphic dark energy models," *Journal of High Energy Physics*, vol. 2011, no. 3, p. 86, 2011.

[48] A. Khodam-Mohammadi, P. Majari, and M. Malekjani, "Agegraphic reconstruction of modified F(R) and F(G) gravities," *Astrophysics and Space Science*, vol. 331, no. 2, pp. 673–677, 2011.

[49] M. H. Daouda, M. E. Rodrigues, and M. J. S. Houndjo, "Static anisotropic solutions in f(T) theory," *European Physical Journal C*, vol. 72, no. 2, pp. 1–12, 2012.

[50] M. J. S. Houndjo and O. F. Piattella, "Reconstructing f(R, T) gravity from holographic dark energy," *International Journal of Modern Physics D*, vol. 21, no. 3, Article ID 1250024, 2012.

[51] M. R. Setare, "Holographic modified gravity," *International Journal of Modern Physics D*, vol. 17, no. 12, pp. 2219–2228, 2008.

[52] M. R. Setare and E. N. Saridakis, "Correspondence between holographic and Gauss-Bonnet dark energy models," *Physics Letters B*, vol. 670, no. 1, pp. 1–4, 2008.

[53] M. R. Setare and M. Jamil, "Correspondence between entropy-corrected holographic and Gauss-Bonnet dark-energy models," *Europhysics Letters*, vol. 92, no. 4, Article ID 49003, 2010.

[54] U. Debnath and M. Jamil, "Correspondence between DBI-essence and modified Chaplygin gas and the generalized second law of thermodynamics," *Astrophysics and Space Science*, vol. 335, no. 2, pp. 545–552, 2011.

[55] S. Chottopadhyay and U. Debnath, "Correspondence between Ricci and other dark energies," *International Journal of Theoretical Physics*, vol. 50, no. 2, pp. 315–324, 2011.

[56] A. Jawad, S. Chattopadhyay, and A. Pasqua, "Reconstruction of f(G) gravity with the new agegraphic dark-energy model," *The European Physical Journal Plus*, vol. 128, p. 88, 2013.

[57] M. Sharif and A. Jawad, "Cosmological evolution of interacting new holographic dark energy in non-flat universe," *The European Physical Journal C*, vol. 72, no. 8, pp. 2097–2098, 2097.

[58] M. Sharif and Abdul Jawad, "Interacting generalized dark energy and reconstruction of scalar field models," *Modern Physics Letters A*, vol. 28, no. 38, Article ID 1350180, 15 pages, 2013.

[59] M. Sharif and A. Jawad, "Reconstruction of scalar field dark energy models in Kaluza-Klein universe," *Communications in Theoretical Physics*, vol. 60, no. 2, p. 183, 2013.

[60] A. Jawad, A. Pasqua, and S. Chattopadhyay, "Correspondence between f(G) gravity and holographic dark energy via power-law solution," *Astrophysics and Space Science*, vol. 344, no. 2, pp. 489–494, 2013.

[61] S. Tsujikawa and M. Sami, "A unified approach to scaling solutions in a general cosmological background," *Physics Letters, Section B: Nuclear, Elementary Particle and High-Energy Physics*, vol. 603, no. 3-4, pp. 113–123, 2004.

[62] S. Mizuno, S.-J. Lee, and E. J. Copeland, "Cosmological evolution of general scalar fields in a brane-world cosmology," *Physical Review D*, vol. 70, no. 4, Article ID 043525, 10 pages, 2004.

[63] C. Armendáriz-Picón, T. Damour, and V. Mukhanov, "k-Inflation," *Physics Letters B*, vol. 458, no. 2-3, pp. 209–218, 1999.

[64] T. Chiba, T. Okabe, and M. Yamaguchi, "Kinetically driven quintessence," *Physical Review D*, vol. 62, Article ID 023511, 2000.

[65] C. Armendáriz-Picón, V. Mukhanov, and P. J. Steinhardt, "Essentials of k-essence," *Physical Review D*, vol. 63, Article ID 103510, 2001.


Journal of Gravity
Journal of Photonics
The Scientific World Journal
Journal of Soft Matter
Advances in Condensed Matter Physics
Journal of Fluids
Journal of Aerodynamics
Hindawi
Submit your manuscripts at
http://www.hindawi.com
International Journal of Statistical Mechanics
International Journal of Optics
Journal of Computational Methods in Physics
Advances in High Energy Physics
Journal of Thermodynamics
Physics Research International
Advances in Astronomy
Journal of Solid State Physics
Journal of Astrophysics
International Journal of Superconductivity
Journal of Biophysics
Journal of Atomic and Molecular Physics